CrossMark

ORIGINAL ARTICLE

Comprehensive analysis of tropomyosin isoforms in skeletal muscles by top-down proteomics

Yutong Jin[1] · Ying Peng[2,3] · Ziqing Lin[2,3] · Yi-Chen Chen[1] · Liming Wei[2,4] ·
Timothy A. Hacker[5] · Lars Larsson[6] · Ying Ge[1,2,3]

Abstract Mammalian skeletal muscles are heterogeneous in nature and are capable of performing various functions. Tropomyosin (Tpm) is a major component of the thin filament in skeletal muscles and plays an important role in controlling muscle contraction and relaxation. Tpm is known to consist of multiple isoforms resulting from different encoding genes and alternative splicing, along with post-translational modifications. However, a systematic characterization of Tpm isoforms in skeletal muscles is still lacking. Therefore, we employed top-down mass spectrometry (MS) to identify and characterize Tpm isoforms present in different skeletal muscles from multiple species, including swine, rat, and human. Our study revealed that Tpm1.1 and Tpm2.2 are the two major Tpm isoforms in swine and rat skeletal muscles, whereas Tpm1.1, Tpm2.2, and Tpm3.12 are present in human skeletal muscles. Tandem MS was utilized to identify the sequences of the major Tpm isoforms. Furthermore, quantitative analysis revealed muscle-type specific differences in the abundance of unmodified and modified Tpm isoforms in rat and human skeletal muscles. This study represents the first systematic investigation of Tpm isoforms in skeletal muscles, which not only demonstrates the capabilities of top-down MS for the comprehensive characterization of skeletal myofilament proteins but also provides the basis for further studies on these Tpm isoforms in muscle-related diseases.

Keywords Tropomyosin · Skeletal muscle · Isoform · Post-translational modification · Top-down mass spectrometry

✉ Ying Ge
ying.ge@wisc.edu

1 Department of Chemistry, University of Wisconsin-Madison, 1101 University Ave., Madison, WI 53706, USA

2 Department of Cell and Regenerative Biology, University of Wisconsin-Madison, 1111 Highland Ave., Madison, WI 53705, USA

3 Human Proteomics Program, University of Wisconsin-Madison, 1111 Highland Ave., Madison, WI 53705, USA

4 Institutes of Biomedical Sciences, Fudan University, Shanghai 200032, P.R. China

5 Department of Medicine, School of Medicine and Public Health, University of Wisconsin-Madison, 1111 Highland Ave., Madison, WI 53705, USA

6 Department of Physiology and Pharmacology, Department of Clinical Neuroscience, Clinical Neurophysiology Section, Karolinska Institutet, 171 77 Stockholm, Sweden

Introduction

Mammalian skeletal muscles are composed of heterogeneous muscle fiber types (Bottinelli and Reggiani 2000; Schiaffino and Reggiani 2011; Scott et al. 2001). This heterogeneity allows skeletal muscles to respond to a variety of functional demands, including sustained low-intensity contractions (e.g. posture keeping), repeated submaximal contractions (e.g. locomotion), and high-intensity or maximal contractions (e.g. jumping) (Bottinelli and Reggiani 2000; Schiaffino and Reggiani 2011). Tropomyosin (Tpm) is a major component of the thin filament in skeletal muscles and, as such, plays an important role in the regulation of muscle contraction and relaxation (Gunning et al. 2008; Janco et al. 2013; Rajan et al. 2010). Tpm molecules exist as coiled coil dimers that are assembled head-to-tail to form polymers along the actin thin filament

🖄 Springer

(Schevzov et al. 2005). In the relaxed state, Tpm, along with the troponin complex, blocks the myosin binding sites on the thin filament, preventing cross-bridge formation and, ultimately, muscle contraction (Gunning et al. 2005). However, when the intracellular Ca^{2+} concentration increases, Ca^{2+} binding to troponin initiates a conformational change in the Tpm-troponin complex that leads to a azimuthal movement of Tpm along the actin filaments (Hitchcock-DeGregori et al. 1973). This positional shift exposes the myosin-binding sites on the actin filament and allows for cross-bridge formation and muscle contraction.

The Tpm protein family is known to be highly complex with a myriad isoforms arising from multiple genes (Denz et al. 2004; Perry 2001; Rajan et al. 2010). In total four different genes encode Tpm isoforms, namely *TPM1*, *TPM2*, *TPM3*, and *TPM4*, each of which gives rise to multiple proteoforms (Smith et al. 2013) via alternative splicing, the selection of alternative promoters, and post-translational modifications (PTMs) (Marston and Redwood 2003; Wieczorek et al. 1988). The *TPM1* gene is composed of 15 exons and encodes the greatest number of Tpm isoforms, including Tpm1.1 (also known as Tpm1.1$_{St(a.b.b.a)}$ or α-Tm) (Geeves et al. 2015) expressed in striated muscles and Tpm1.3 present in smooth muscles (Perry 2001). Other major Tpm isoforms expressed in striated and smooth muscles are Tpm2.2 (also known as Tpm2.2$_{St(a.b.b.a)}$ or β-Tm) and Tpm2.1, respectively, which are both encoded by *TPM2* (Rajan et al. 2010). Additional Tpm isoforms, including Tpm3.12 (also known as Tpm3.12$_{St(a.b.b.a)}$ or γ-Tm) and Tpm4.1 (also known as Tpm4.1$_{cy(a.b.b.d)}$ or δ-Tpm), are encoded by *TPM3* and *TPM4*, respectively; however, Tpm3.12 is believed to be expressed only in slow-twitch skeletal muscles (Kee and Hardeman 2008; Perry 2001), while Tpm4.1 is detected in both slow and fast twitch muscles (Kee and Hardeman 2008; Wang et al. 2008).

Given the essential roles of Tpm in regulating muscle contraction, a variety of muscle-related diseases associated with mutations of Tpm encoding gene and expression of Tpm isoforms have been reported (Scellini et al. 2015; Tajsharghi et al. 2012). For example, Memo and Marston observed various mutations in Tpm in the actin-Tpm interface and the mutation of amino acids in Tpm can cause a loss-of-function in skeletal muscles (Memo and Marston 2013). In addition, Clarke et al. discovered that the mutation in exon 4 of *TPM2* gene which encodes Tpm2.2 is the genetic cause of cap disease (Clarke et al. 2009). Moreover, EI-Mezgueldi et al. demonstrated that the transitions between the inactive and active states of thin filaments are affected by the skeletal muscle myopathy mutations in *TPM3* gene of Tpm (El-Mezgueldi et al. 2014). Hence, a systematic assessment of the composition and the relative abundance of Tpm isoforms and their PTMs in skeletal muscles is important but remains lacking.

Top-down mass spectrometry (MS) is a powerful tool for the comprehensive characterization of protein isoforms arising from multiple genes, as well as proteoforms resulting from protein PTMs and sequence variations (Ayaz-Guner et al. 2009; Chait 2006; Dong et al. 2012; Ge et al. 2009; Peng et al. 2012; Zabrouskov et al. 2008). Different from the traditional bottom-up method, top-down MS analyzes intact proteins without digestion, thereby providing a bird's eye-view of all isoforms encoded by different genes together with their associated proteoforms as a result of alternatively spliced RNA transcripts and PTMs (Smith et al. 2013). Following MS analysis, individual protein species of interest can be subjected to dissociation by tandem MS (MS/MS) techniques, including, but not limited to, electron capture dissociation (ECD) (Zubarev et al. 2000) and collisionally activated dissociation (CAD) (Senko et al. 1994). Analysis of the resulting fragments allows for the localization of sequence variations and PTMs within the sequence of the intact protein. Our group has previously studied Tpm isoforms in swine (Peng et al. 2013a) and human (Peng et al. 2013b) cardiac muscles by top-down MS, using an offline multi-step purification strategy. Recently, we have developed a simple and robust top-down liquid chromatography (LC)/MS+ (Thangaraj et al. 2010; Whitelegge et al. 2002) strategy for the analysis of myofilament proteins extracted from cardiac tissues (Chen et al. 2015; Peng et al. 2014), which greatly simplified the purification procedure of myofilament proteins. Herein, we have employed this strategy to characterize Tpm isoforms present in different types of skeletal muscle from three species (swine, rat, and human) toward a better understanding of the functional role of Tpm in skeletal muscles.

Experimental section

Chemical and reagents

All reagents were obtained from Sigma-Aldrich (St. Louis, MO, USA) unless noted otherwise. All buffer solutions were prepared in Milli-Q water (Millipore, Corp., Billerica, MA, USA) and mobile phases were prepared in HPLC grade water (Thermo Fisher Scientific, Fair Lawn, NJ, USA).

Skeletal muscle tissue samples

Swine skeletal muscle tissues were obtained from healthy juvenile Yorkshire domestic swine from the University of Wisconsin-Madison colony. Rat skeletal muscle tissues were excised from the gastrocnemius, diaphragm, and soleus from three healthy rats (Hsd: Sprague–Dawley SD,

Harlan Laboratories, Indianapolis, IN, USA). Human skeletal muscle biopsies were collected from the vastus lateralis and the tibialis anterior from two young healthy women. Swine and rat tissues were snap frozen in liquid nitrogen and stored in a −80 °C freezer and human tissues were snap frozen in liquid propane chilled by liquid nitrogen and stored in a −140 °C freezer. All procedures were approved by UW-Madison Animal Care and Use Committee and the ethical committee of the Uppsala University. Human tissue samples were carried out according to the guidelines of the Declaration of Helsinki.

Purification of Tpm

A rapid purification method, employing 2-[4-(2-hydroxyethyl)piperazin-1-yl]ethanesulfonic acid (HEPES) and 1 % trifluoroacetic acid (TFA) extraction buffer (Peng et al. 2013a) together with on-line LC/MS system was utilized to purify Tpm from skeletal muscle from a variety of sources (Figure S1). Approximately 8 mg of skeletal muscle tissue was homogenized for ∼2 min in 80 μL of HEPES extraction buffer (HEPES 25 mM pH 7.5, ethylenediaminetetraacetic acid (EDTA) 2.5 mM, NaF 50 mM, phenylmethylsulfonyl fluoride (PMSF) (in isopropanol) 0.25 mM and Na_3VO_4 0.25 mM) using a Teflon homogenizer (1.5 mL tube Rounded tip, Scienceware, Pequannock, NJ, USA). The homogenate was centrifuged at 16,100 rcf for 20 min at 4 °C (Sorvall Legend Micro 21R, Thermo Fisher Scientific, Am Kalkbarg, Germany) and the supernatant was discarded. The pellet was then re-homogenized for ∼2 min in 80 μL of TFA extraction buffer [1 % TFA, 1 mM Tris(2-carboxyethyl)phosphine (TCEP)] to extract myofilament proteins including Tpm. The resulting homogenate was then centrifuged at 16,100 rcf at 4 °C for 20 min. The supernatant was centrifuged again at 16,100 rcf at 4 °C for an additional 20 min to completely remove particulate matter prior to LC/MS. The remaining pellet after the TFA extraction was dissolved using 80 μL SDS sample buffer (50 mM Tris–HCl, pH 6.8, 2 % SDS, 10 % glycerol, 1 % β-mercaptoethanol, 0.05 % bromophenol blue), and boiled at 95 °C for 10 min, followed by sonication for 5 min. The myofilament mixture in the supernatant was separated by a home-made reversed-phase column (polymeric reversed-phase spherical, PLRP-S, 200 mm × 500 μm, 10 μm, 1,000 Å, PLRP-S particles were purchased from Varian, Lake Forest, CA, USA) in a 2D-nano LC system (Eksigent, Dublin, CA, USA). Separated proteins were analyzed by an online linear ion trap mass spectrometer (LTQ, Thermo Scientific Inc., Bremen, Germany). All myofilament proteins were separated and eluted using a 57-min gradient and a flow rate of 12.5 μL/min (mobile phase A: 0.1 % formic acid in water; mobile phase B: 0.1 % formic acid in 50:50 acetonitrile and

ethanol). The gradient increases from 20 % mobile phase B to 95 % mobile phase B in first 43 min and then decreases to 20 % mobile phase B and keeps at 20 % in the next 14 min. Fractions containing Tpm were collected in microcentrifuge tubes when eluted out from the column at ∼25–26.5 min retention time and stored at −80 °C for offline high-resolution MS and MS/MS analyses. Bicinchoninic acid (BCA) protein assays were performed to measure protein concentration of the myofilament extract (in 1 % TFA) and the HPLC-purified Tpm. The HEPES extraction, TFA extraction, the pellet (dissolved in SDS sample buffer) were analyzed using SDS-PAGE and Western Blot to evaluate the extraction efficiency. Briefly, 6 μL of each of the HEPES, TFA and pellet fractions were loaded into 15 % SDS polyacrylamide gel for electrophoretic separation, followed by Western Blot analysis using 1:1000 dilution of Anti-TPM1 antibody (Abcam, Cambridge, MA, USA). Detection of Tpm was carried out using enhanced chemiluminescence reagent (Pierce, Thermo Scientific, Rockford, IL, USA). Similarly, 6 μL of each of the HEPES, TFA and pellet fractions, as well as the HPLC-purified Tpm were loaded into 15 % SDS polyacrylamide gel for electrophoretic separation, followed by Coomassie Blue staining.

Top-down MS and MS/MS analyses

Purified Tpm from skeletal muscles was analyzed in a 7T LTQ/Fourier transform ion cyclotron resonance (LTQ/FT-ICR) mass spectrometer (Thermo Scientific Inc., Bremen, Germany) coupled with an automated chip-based nano-electrospray ionization (nanoESI) source (Triversa Nano-Mate; Advion Biosciences, Ithaca, NY, USA). The spray voltage used to infuse Tpm into the mass spectrometer was 1.3–1.4 kV versus the inlet of the mass spectrometer, producing a flow rate of 50–200 nL/min. The resolution of the FT-ICR was set to 200,000 (at m/z of 400). Automatic gain control for a full scan in the LTQ cell, FT-ICR cell, MS^n FT-ICR cell, and ECD was set to 3×10^4, 5×10^5, 9×10^5 and 9×10^5, respectively. For MS/MS analyses, a normalized collision energy of 21–25 % was used for CAD and an electron energy of 2.0–3.0 % (0.8–1.8 eV according to the offset of 3.8 eV) with a 70 ms duration and no additional delay were used for ECD. Generally, 1000–3000 scans were averaged to produce high quality CAD and ECD spectra.

Data analysis

All MS and MS/MS data were analyzed using in-house developed MASH Suite software (version 1.2) (Guner et al. 2014), which uses the THRASH (Horn et al. 2000) algorithm for spectral deconvolution. A signal to noise (S/N)

threshold of 3 and a minimum fit of 60 % were used for program processing and manual validation was performed to ensure data accuracy. The fragment ions in the tandem mass spectra were assigned based on the protein sequence of Tpm isoforms in Swiss-Prot protein knowledgebase (Unit-ProtKB/Swiss-Prot). Allowance was made for possible PTMs, including N-terminal acetylation and phosphorylation, as well as amino acid polymorphisms. A 10 ppm cutoff was used for the assignment of fragment ions. To confirm or exclude the existence of phosphorylation sites on certain fragments, the masses of fragment ions were manually validated with a mass discrepancy of ~ 80 Da. The reported molecular masses are the most abundant mass for intact proteins and the monoisotopic mass for fragment ions.

Quantitative analysis of Tpm isoforms and their associated PTMs in swine, rat, and human skeletal muscle samples was performed using peak intensities from the high-resolution FT-ICR mass spectra as previously described (Peng et al. 2013a). Briefly, the sum of the peak heights of the top three isotopomers was used to calculate the relative abundance of each isoform/proteoform. The percentage of each individual isoform/proteoform was defined as summed abundances of the isoform/proteoform over the summed abundances of the entire Tpm population. All data are expressed as mean $\pm$ standard error of mean (SEM).

Results and discussion

An integrated workflow for myofilament extraction, Tpm purification and characterization

The entire workflow of our top-down LC/MS+ strategy includes myofilament protein extraction, online LC/MS separation along with simultaneous fraction collection of purified Tpm for subsequent comprehensive protein characterization by offline high-resolution MS/MS (Figure S1). In contrast to our previously developed multi-step purification strategy for the characterization of Tpm isoforms in swine (Peng et al. 2013a) and human (Peng et al. 2013b) heart muscles, this LC/MS+ approach is much more robust and significantly simplifies the protein purification procedure and minimizes sample consumption.

The myofilament extraction method employed in this study was based on a previous method developed by Van Eyk and co-workers (Arrell et al. 2001; Neverova and Van Eyk 2002). It consists of two extraction steps: first extraction using HEPES buffer at neutral pH to extract cytosolic proteins and the second extraction using 1 % TFA (pH 2.2) to extract myofilament proteins from the remaining pellet of the first extraction. Myofilament proteins such as actin, troponin and Tpm are enriched in this TFA extraction since the majority of the myofilament proteins are soluble at the acidic pH, as demonstrated previously (Neverova and Van Eyk 2002). To evaluate the extraction efficiency of myofilament proteins, we have performed a BCA protein assay on the myofilament extraction (in 1 % TFA). The protein assay showed that approximately 40–50 μg myofilament proteins was extracted from 1 mg tissue (~ 40–50 μg/mg). Thus, our myofilament extraction protocol has similar efficiency as those reported previously (Canton et al. 2004; Jin and Lin 1988).

The TFA extraction containing the enriched myofilament proteins is then separated on HPLC and the fraction containing purified Tpm is collected for comprehensive MS analysis. To further evaluate the extraction efficiency of the purified Tpm, we have performed SDS-PAGE and Western Blot analysis of the HEPES extraction, TFA extraction, the pellet (dissolved in SDS sample buffer) and the purified Tpm from swine skeletal muscle (Figure S2). The SDS-gel demonstrated that myofilament proteins are significantly enriched in the TFA extraction and high purity Tpm was obtained from the collected LC fraction (Figure S2a). The identity and relative quantity of Tpm in the HEPES extraction, TFA extraction and pellet were further confirmed by Western Blot (Figure S2b). Moreover, we have determined the concentration of the purified Tpm to be ~ 2 μg/mg tissue by a BCA protein assay, which corresponds to approximately 30 % of the total amount Tpm from swine skeletal muscle tissue. This is consistent with the extraction efficiency of previous Tpm purification methods (Bailey 1948).

Top-down MS analysis of major Tpm isoforms in swine skeletal muscles

We have employed the LC/MS+ strategy to analyze Tpm isoforms purified from swine skeletal muscles. All detectable Tpm isoforms present in swine skeletal muscles were fraction collected and subjected to top-down MS analysis. High-resolution MS analysis of Tpm extracted from swine skeletal muscle tissues revealed the presence of two Tpm isoforms with molecular masses of 32736.11 and 32877.99 Da (Fig. 1a). However, neither of these molecular masses matches with the theoretical molecular masses of either Tpm1.1 or Tpm2.2 calculated based on their DNA-encoded amino acid sequences.

A thorough sequence homology analysis among all the possible swine Tpm1.1 sequences available was first carried out to search for close matches in the Swiss-Prot database. The closest match for the experimental molecular mass of 32736.11 Da was 32705.75 Da (UnitprotKB/ Swiss-Prot P42639, TPM1_PIG), which was calculated
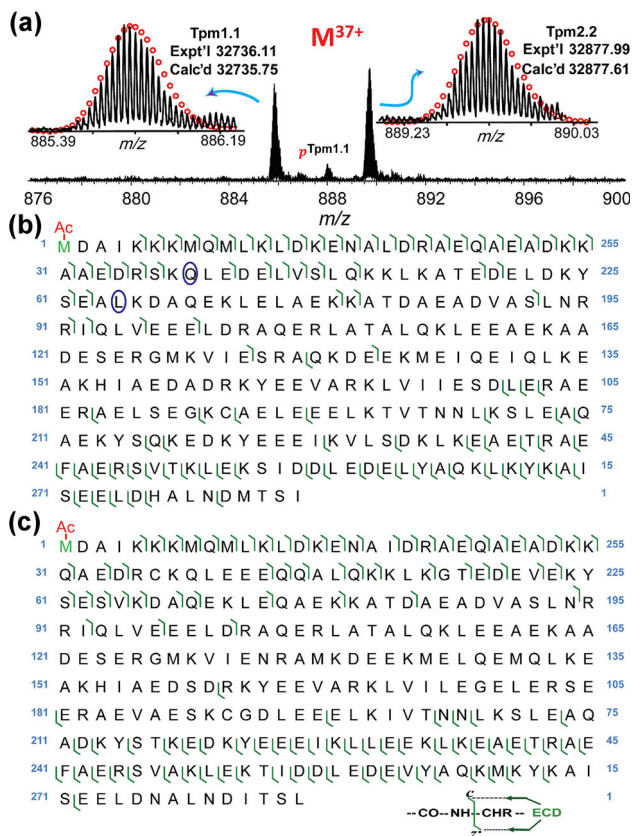
Fig. 1 a High-resolution spectra of Tpm isoforms and mono-phosphorylated Tpm1.1 purified from swine skeletal muscles. The molecular weight of Tpm1.1 was calculated based on the DNA-predicted sequence (UnitprotKB/Swiss-Prot P42639, TPM1_PIG) with N-terminal acetylation and two amino acid polymorphisms, R38 → Q (−28.04) and P64 → L (16.03). The molecular weight of Tpm2.2 was calculated on the basis of DNA-predicted sequence (UnitprotKB/Swiss-Prot P58774, TPM2_MOUSE) with N-terminal acetylation. *pTpm1.1* mono-phosphorylated Tpm1.1, *red circles* theoretical isotopic abundance distribution of the isotopomer peaks corresponding to the assigned mass, *Calc'd* calculated most abundant molecular weight, *Expt'l* experimental most abundant molecular weight. b ECD fragment map of swine skeletal Tpm1.1 with N-terminal acetylation and two amino acid polymorphisms R38 → Q and P64 → L (*blue circles*). Fragment assignments were made to the DNA-predicted sequence of swine Tpm1.1 (UnitprotKB/Swiss-Prot P42639, TPM1_PIG). c ECD fragment map of swine skeletal Tpm2.2 with acetylation of the N-terminus. Fragment assignments were made to the DNA-predicted sequence of mouse Tpm2.2 (UnitprotKB/Swiss-Prot P58774, TPM2_MOUSE)

based on the sequence of the *TPM1* gene with a mass discrepancy of 30.36 Da. The mass shift of 30.36 Da does not match any single modification, suggesting that a combination of modifications may be present in this isoform. MS/MS analysis was performed on precursor ions of tentatively assigned Tpm1.1 (32736.11 Da) at the multiple charge states. According to the ECD spectra of Tpm1.1, only 51 $z\cdot$ ions were assigned based on the swine Tpm1.1 sequence from the database (UnitprotKB/Swiss-Prot

P42639, TPM1_PIG). The observation that no c ions matched the predicted values in the database suggested a potential modification at the N-terminus. After considering N-terminal acetylation, which is a common modification in eukaryotic proteins, a total of 32 c ions could be assigned. There were no matches of c ions yet observed after Arg38. However, 10 more fragment c ions in ECD appeared to have a mass decrease of 28.04 Da compared to the calculated c ions after Arg38, which confirms an amino acid polymorphism of Arg38 → Gln38 with a mass discrepancy of 28.04 Da. Moreover, after considering a mass increase of 16.03 Da after Pro64, 9 more c ions were identified, revealing an amino acid polymorphism of Pro64 → Leu64. With the consideration of all three modifications, the calculated molecular mass of swine Tpm1.1 of 32735.75 Da (32705.75 + 42.01 − 28.04 + 16.03 = 32735.75) matches the experimental value of 32736.11 Da, which is consistent with our previous studies on swine cardiac muscles (Peng et al. 2013a). The ECD spectra showed a total of 51 $z\cdot$ ions and 51 c ions matched with the modified Tpm1.1 sequence (Fig. 1b). The peak next to Tpm1.1 with a molecular mass of 32816.12 Da was tentatively assigned as the mono-phosphorylated Tpm1.1 since it has a mass discrepancy of 80.01 Da compared to the un-phosphorylated Tpm1.1. MS/MS was also performed on the mono-phosphorylated Tpm1.1. However, due to the low intensity of this proteoform, the phosphorylation site could not be localized.

The other major peak with molecular mass of 32877.99 Da has a mass discrepancy of 141.88 Da from Tpm1.1. Nevertheless, the sequence homology analysis indicates that the sequence of this isoform does not match any of the swine Tpm sequence in the Swiss-Prot sequence even after considering modifications. With similar strategy mentioned in the last paragraph, this isoform was confirmed as swine Tpm2.2 with the exact same sequence of mouse Tpm2.2 (UnitprotKB/Swiss-Prot P58774, TPM2_MOUSE) encoded by *TPM2* gene with an acetylation on the first amino acid (42.01 Da) at the N-terminus. The ECD spectra generated 54 c ions and 56 $z\cdot$ ions corresponding to the predicted sequence (Fig. 1c).

Moreover, we analyzed three technical replicates of swine skeletal muscle tissues to test the reproducibility of this top-down MS method. In this case, highly reproducible mass spectra for swine skeletal Tpm from the replicates were obtained (Figure S3) except for a small proportion of noncovalent phosphoric acid adduct from Tpm1.1 and oxidation of Tpm2.2, which was commonly observed for MS analysis of intact proteins (Peng et al. 2013a). This result demonstrates the feasibility of our approach for the purpose of the relative quantitation of Tpm isoforms in various muscle types among multiple species.

Top-down MS analysis of major Tpm isoforms in rat skeletal muscles

To explore the variations of Tpm isoforms among different species, we analyzed the Tpm forms from rat skeletal muscles (Fig. 2). High-resolution MS analysis of the Tpm extracted from rat gastrocnemius, diaphragm, and soleus muscles revealed the presence of two major Tpm isoforms in all rat skeletal muscle types with molecular masses of 32722.36 and 32878.23 Da (Fig. 2a). It is clear that all three muscle types have the same major Tpm isoforms,
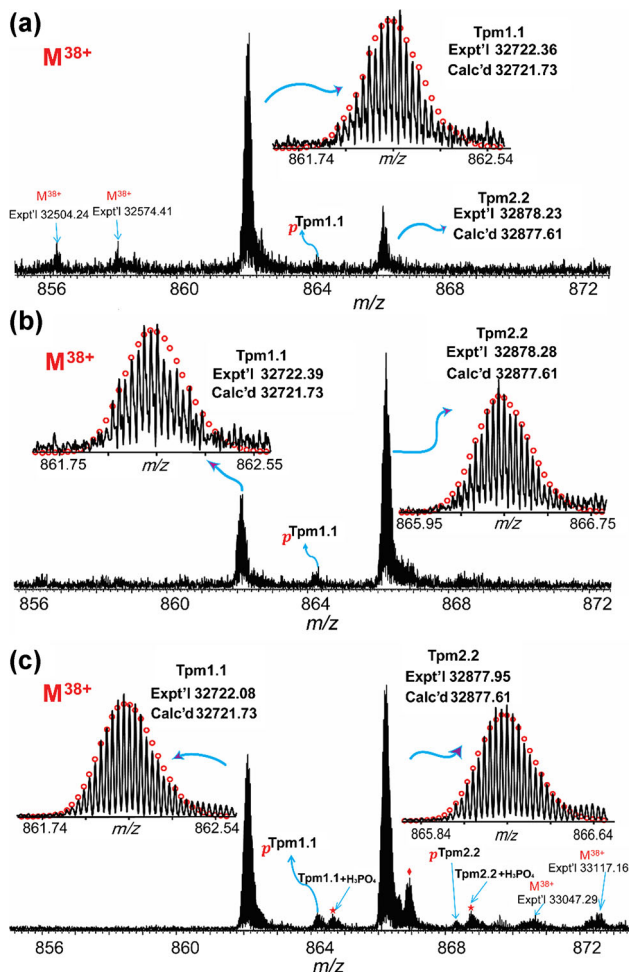
tentatively assigned as Tpm1.1 and Tpm2.2, based on their almost identical molecular masses.

To further confirm the identities of the major Tpm isoforms in rat skeletal muscles, we utilized the same method as described in the previous section. The experimental molecular masses of 32722.36 and 32878.23 Da match closest to the calculated molecular mass of 32679.72 Da of rat Tpm1.1 (UnitprotKB/Swiss-Prot P04692, TPM1_RAT) and 32836.60 Da of rat Tpm2.2 (UnitprotKB/Swiss-Prot P58775, TPM2_RAT), respectively, with a mass discrepancy of ∼42 Da. Given the fact that N-terminal acetylation creates an exact molecular mass increase of 42.01 Da, we hypothesized those two isoforms as N-terminal acetylated Tpm1.1 and Tpm2.2. To validate our hypothesis, MS/MS was performed on these two major Tpm isoforms of all three muscle types to determine the sequences and modifications. Both ECD and CAD analyses were carried out on the precursor ions of rat Tpm1.1 and Tpm2.2 for all three muscle types at the specific charge states. Significantly more fragments were assigned after N-terminal acetylation was considered for both Tpm1.1 and Tpm2.2. A total of 66 c ions and 49 $z\cdot$ ions from ECD spectra and 55 b ions and 34 y ions from CAD spectra match the predicted values of the modified Tpm1.1 sequence (Fig. 3a). 56 c ions, 56 $z\cdot$ ions,

Fig. 2 High-resolution spectra of Tpm isoforms and their PTMs in rat skeletal muscles with three muscle types: a gastrocnemius, b diaphragm and c soleus. Molecular weights were calculated based on the DNA-predicted sequence (UnitprotKB/Swiss-Prot P04692, TPM1_RAT for Tpm1.1 and UnitprotKB/Swiss-Prot P58775, TPM2_RAT for Tpm2.2) with N-terminal acetylation. $pTpm1.1$ monophosphorylated Tpm1.1, red circles theoretical isotopic abundance distribution of the isotopomer peaks corresponding to the assigned mass; red star noncovalent adduct of phosphoric acid ($+H_3PO_4$), red diamond a potential new unknown isoform of Tpm in rat soleus muscle, Calc'd calculated most abundant molecular weight, Expt'l experimental most abundant molecular weight
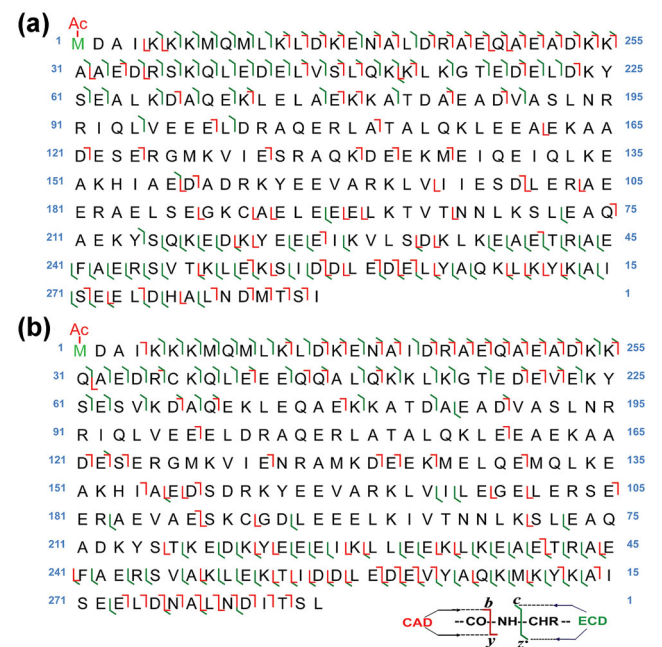

Fig. 3 a ECD/CAD fragment maps of rat Tpm1.1. Fragment assignments were made based on the DNA-predicted sequence of rat Tpm1.1 (UnitprotKB/Swiss-Prot P04692, TPM1_RAT) with N-terminal acetylation. b ECD/CAD fragment maps of rat Tpm2.2. Fragment assignments were made based on the DNA-predicted sequence of rat Tpm2.2 (UnitprotKB/Swiss-Prot P58775, TPM2_RAT) with N-terminal acetylation

59 b ions and 32 y ions were assigned for rat Tpm2.2 (Fig. 3b). The representative fragment ions of rat Tpm1.1 and Tpm2.2 are shown in Figure S4.

Several minor Tpm isoforms and possibly their PTMs (same charge state as the major Tpm) are also present with lower intensities among the muscle types (Fig. 2). Mono-phosphorylation, phosphoric acid adduct, oxidation were tentatively assigned based on their mass shifts of ~80, 98, and 16 Da, respectively, corresponding to Tpm1.1 and Tpm2.2. There are also other minor peaks carrying the same charge as Tpm1.1 and Tpm2.2 but no direct matches for the mass shifts could be obtained (Fig. 2a, c). We also tried our best to identify these isoforms, but unfortunately the intensities of these minor peaks were too low to yield enough fragments in MS/MS for deep sequencing and modification characterization. We envision the sensitivity of this LC–MS+ method could be improved with the use of more sensitive mass spectrometers as well as the new developments on the ion isolation and dissociation techniques. Note that the LTQ/FT mass spectrometer used in this study is 8-year-old and there are now new generation of high-resolution high sensitivity FT-ICR and Orbitrap mass spectrometers available (Eliuk and Makarov 2015; Hendrickson et al. 2015; Kostyukevich et al. 2012; Xian et al. 2012). In addition, only a single charge state can be isolated for sequencing using the current LTQ/FT mass spectrometer. The ion intensity of a specific charge state is rather low to yield enough fragment ions for sequencing. One possible solution for this limitation is to accumulate ions from different charge states to a specific one by ion parking (Holden et al. 2016; Huang and McLuckey 2010). The intensity was reported to have an increase of at least ten times. Recently, Holden et al. has demonstrated the high promise of integration of ion parking with ultraviolet photodissociation (a relatively new and powerful tandem mass spectrometry technique) for intact protein analysis (Holden et al. 2016).

Top-down MS analysis of major Tpm isoforms in human skeletal muscles

Three major isoforms with molecular mass of 32750.26, 32860.37 and 32892.20 Da were detected in the high-resolution mass spectra of human Tpm from the vastus lateralis and tibialis anterior muscles (Fig. 4). To map the sequences of human Tpm isoforms, sequence homology analysis was performed using all available human Tpm sequences in the Swiss-Prot database. The human Tpm isoform with molecular mass of 32750.26 Da was identified as human Tpm1.1 (UnitprotKB/Swiss-Prot P09493, TPM1_HUMAN) with N-terminal acetylation. Due to the limited amount of human sample and the relative low signal of this isoform, the ECD and CAD spectra generated only 39 c ions and 3 $z\cdot$ ions as well as 7 b ions and 11
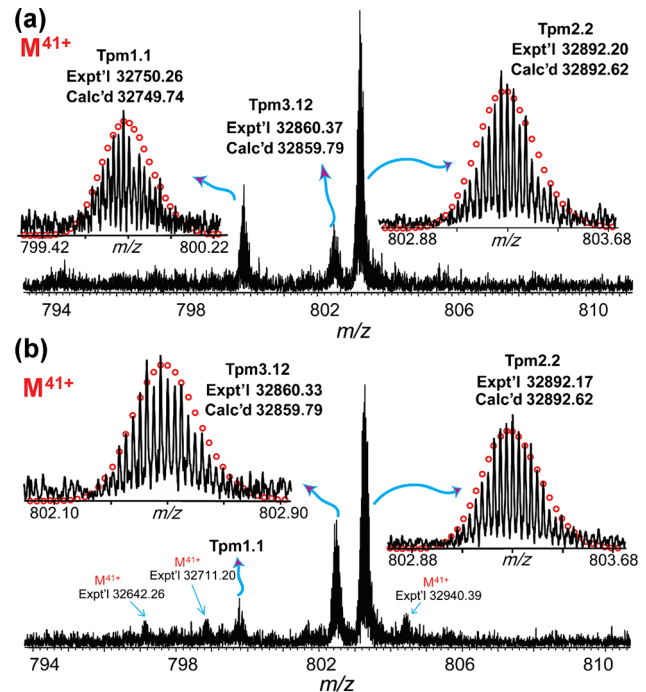

Fig. 4 High-resolution spectra of Tpm isoforms in human skeletal muscle biopsies with two muscle types: **a** vastus lateralis and **b** tibialis anterior. Molecular weights were calculated based on the DNA-predicted sequence (UnitprotKB/Swiss-Prot P09493 TPM1_HUMAN for Tpm1.1, UnitprotKB/Swiss-Prot P07951 TPM2_HUMAN for Tpm2.2, and UnitprotKB/Swiss-Prot P06753 TPM3_HUMAN for Tpm3.12) with N-terminal acetylation

y ions, respectively, according to the acetylated human Tpm1.1 sequence (Fig. 5a). The experimental molecular mass matches the calculated value well, which indicates this isoform as the modified human Tpm1.1 despite of the relatively low sequence coverage. After considering an acetylation at the N-terminus, the experimental molecular mass of the other major Tpm form (32892.20 Da) was identified as human Tpm2.2 (UnitprotKB/Swiss-Prot P07951, TPM2_HUMAN). The ECD and CAD data of protein precursor ions (38^+, 39^+, 40^+, 41^+) of human Tpm2.2 confirmed the sequence with N-terminal acetylation. A total of 42 c ions and 52 $z\cdot$ ions were detected in ECD spectra as well as 27 b ions and 21 y ions in CAD spectra (Fig. 5b).

Interestingly, an additional major peak with molecular mass of 32860.37 Da was observed with a mass discrepancy of 110.11 Da compared to human Tpm1.1 peak (Fig. 4a). After removing the first amino acid Met-1 and adding acetylation at second amino acid Met-2 from N-terminus, the calculated molecular mass of human Tpm3.12 32859.79 Da (UnitprotKB/Swiss-Prot P06753, TPM3_HUMAN) matches the experimental molecular mass of this peak. Hence we assigned it as human Tpm3.12 based on its accurate molecular mass measurement.
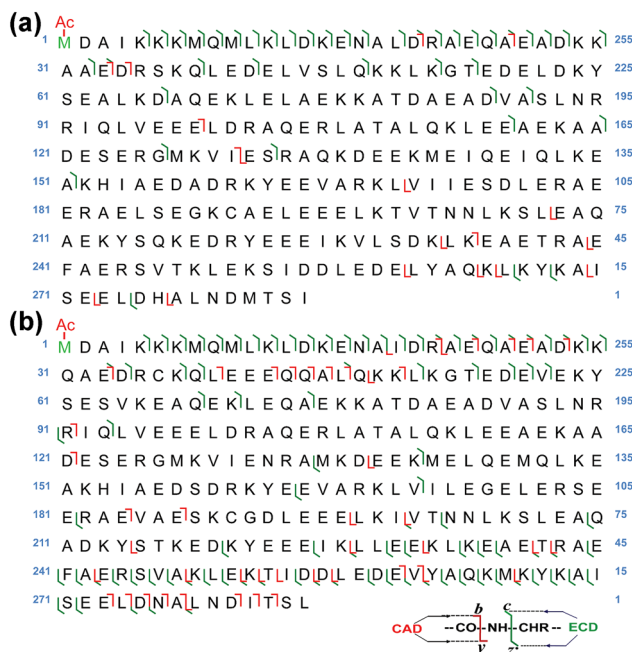
(a)

(b)

Fig. 5 a ECD/CAD fragment maps of human Tpm1.1. Fragment assignments were made to the DNA-predicted sequence of human Tpm1.1 (UnitprotKB/Swiss-Prot P09493, TPM1_HUMAN) with N-terminal acetylation. **b** ECD/CAD fragment maps of human Tpm2.2. Fragment assignments were made to the DNA-predicted sequence of human Tpm2.2 (UnitprotKB/Swiss-Prot P07951, TPM2_HUMAN) with N-terminal acetylation

Nevertheless, the fragments in MS/MS (data not shown) were not enough to confirm this Tpm as human Tpm3.12 with high confidence due to the limited amount of human biopsy tissue. Other minor peaks were also observed in Fig. 4b. These peaks were eluted at the same retention time and were present for all charge states, which indicates they belong to the Tpm isoforms but the relative abundances are rather low.

Sequence alignment of Tpm isoforms from different species

According to the results presented here (Figs. 1, 2, and 4), Tpm isoforms and their PTMs, including Tpm1.1, mono-phosphorylated Tpm1.1, Tpm2.2, and Tpm3.12, are present in multiple species and muscle types. The sequences of Tpm isoforms and PTMs were characterized by top-down MS (Figs. 1, 3, and 5). The sequence alignment of Tpm isoforms (Figure S5) in skeletal muscles of multiple species shows that Tpm isoforms among different species are highly conserved. In the study of Tpm1.1, two potential amino acid polymorphisms of swine skeletal Tpm1.1 at position 38 (Arg → Gln) and 64 (Pro → Leu) were identified in the sequence (Fig. 1b). Comparison of the modified sequences of Tpm from different species in Figure S5

indicates that Tpm1.1 chains encoded by *TPM1* only have two amino acid substitutions (position 52 and 220 from the N-terminus) among swine, rat and human, while Tpm2.2 chains, which are encoded by *TPM2*, have only one amino acid substitution at position 66 from the N-terminus among three species. The percentages of sequence similarity among the three species are 99.3 and 99.6 % for Tpm1.1 and Tpm2.2, respectively, which highlights the high sequence conservation of Tpm isoforms across different mammalian species. The sequences of Tpm isoforms and similarities among them agree well with our previous studies of Tpm isoforms in swine (Peng et al. 2013a) and human (Peng et al. 2013b) heart tissues.

We also observed N-terminal acetylation of all Tpm chains in this study. The majority of eukaryotic proteins are acetylated at the N-terminus (Driessen et al. 1985). It was demonstrated that without N-terminal acetylation, the actin-binding and polymerization abilities of Tpm are severely impaired (Hitchcock-DeGregori and Heald 1987). It was also reported that unacetylated Tpm has a non-helical conformation at first two N-terminal residues which is not able to form a head-to-tail structure (Greenfield et al. 1998). Three-dimensional structure analysis of Tpm N-terminus showed that acetylation extends the α-helical conformation to the initial Met-1 residue to form a coiled-coil structure (Brown et al. 2001).

Relative quantitation of Tpm isoforms and PTMs

The relative abundances of skeletal Tpm isoforms vary in different muscle types as shown in Fig. 2 (three rat muscle types) and Fig. 4 (two human muscle types). To further determine the composition of Tpm isoforms and their proteoforms in muscle types among different species, the relative abundances of Tpm isoforms/proteoforms were calculated based on high-resolution FT-MS data in Fig. 6. Taking rat skeletal muscle as an example, the percentages of Tpm1.1 in rat gastrocnemius (Fig. 6b), diaphragm (Fig. 6c) and soleus (Fig. 6d) were 74 ± 3, 34 ± 4 and 34 ± 7 %, respectively. Meanwhile, 17 ± 2, 61 ± 3 and 63 ± 8 % of the overall Tpm were observed as Tpm2.2 in rat gastrocnemius, rat diaphragm, and rat soleus, respectively. Specific percentages of all major Tpm isoforms/proteoforms in different muscle types for the three mammalian species can be found in Table S1. Although other minor Tpm isoforms exist in several muscle types among all three species, they have little contribution in the quantitation due to their low abundances. These statistical results confirm that the composition of different Tpm isoforms and their PTMs is muscle-type specific in rat and human skeletal muscles. Different Tpm compositions were observed among swine, rat and human muscles, which
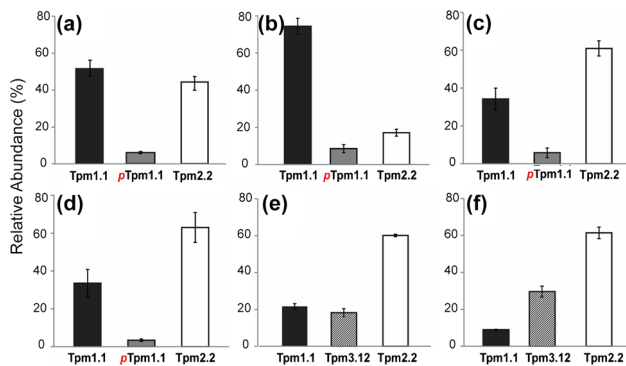
Fig. 6 Relative quantitation of major Tpm isoforms and mono-phosphorylated Tpm1.1 present in skeletal muscles from three species. The percentage of an individual isoform was defined as summed abundances of this isoform/PTM over the summed abundances of the entire Tpm population (n, biological replicates). **a** Swine skeletal muscles, n = 2. Rat skeletal muscles with three muscle types, **b** gastrocnemius, **c** diaphragm and **d** soleus, n = 3. Human skeletal muscle with two muscle types, **e** vastus lateralis, and **f** tibialis anterior, n = 2. Data are expressed as mean ± standard error of mean (SEM)

might result from different muscle types used in each species.

In previous study of rat skeletal muscles, Carraro et al. used two-dimensional gel electrophoresis to quantify the relative abundances of Tpm1.1 and Tpm2.2 in rat soleus and diaphragm (Carraro et al. 1981). Their results showed that the ratio of Tpm1.1: Tpm2.2 in rat soleus is 0.26:1 and that in rat diaphragm is 0.99:1. However, our results show the ratio of Tpm1.1: Tpm2.2 in rat soleus is 0.59:1 and that in rat diaphragm is 0.68:1 with mono-phosphorylated Tpm1.1 included in overall Tpm1.1. The discrepancy is possibly due to the use of different methods (2D gel vs. MS) and there might also be a difference in the age and strain used. Nevertheless, our results show an increasing percentage of Tpm1.1: Tpm2.2 ratio in rat diaphragm compared to soleus, which agrees with the trend in the study by Carraro et al. (1981). The ratio of Tpm1.1:Tpm2.2 in rat soleus muscle is also evaluated by 1D SDS-PAGE. The SDS gel shows a significantly darker band of Tpm2.2 compared to Tpm1.1 in two rat soleus biological replicates (Figure S6), which is consistent with our MS results.

Furthermore, some studies have suggested that muscle functions are related to Tpm isoform compositions (Perry 2001). Four Tpm genes (*TPM1*, *TPM2*, *TPM3*, and *TPM4*) have been identified so far and various isoforms are expressed by different encoding genes, along with alternative RNA processing and splicing (Pittenger et al. 1994). Heterogeneous isoforms play critical roles in controlling muscle contractions and physiological functions (Perry 2001). Tpm1.1 and Tpm2.2 are two major isoforms in skeletal muscles (Cummins and Perry 1974). Generally,

fast fibers contain higher relative abundance of Tpm1.1 (Heeley et al. 1983; Romeroherrera et al. 1982). In our study, human vastus lateralis has higher relative amount of Tpm1.1 (22 %) than that in tibialis anterior (9 %), which strongly supports previous studies showing that the vastus lateralis contains more fast fibers than slow fibers while tibialis anterior is made up of mostly slow twitch muscle fibers (Johnson et al. 1973). More importantly, we have observed Tpm3.12 in both human tissue types and the relative abundance of Tpm3.12 is higher in tibialis anterior than in vastus lateralis. Tpm3.12 is known to be only expressed in slow-twitch skeletal muscles (Perry 2001; Wieczorek et al. 1988). Therefore the assigned human Tpm3.12 is further confirmed since it has a higher percentage in human tibialis anterior (~70 % slow-twitch fibers) compared to that in vastus lateralis (~30 % slow-twitch fibers) based on the analysis of myosin heavy chain isoform expression (data not shown). Interestingly a recent study by Marston et al. observed the presence of Tpm3.12 in human cardiac muscle (Marston et al. 2013).

The ratio of Tpm1.1:Tpm2.2 appears to be muscle-type dependent based on our results and previous studies (Carraro et al. 1981; Lees-Miller and Helfman 1991; Peng et al. 2013a). Previous studies have demonstrated that Tpm1.1 isoform is dominant in cardiac and fast twitch skeletal muscles whereas Tpm2.2 isoform is prominent in slow twitch muscles (Lees-Miller and Helfman 1991). In our previous study of Tpm in swine heart, much more Tpm1.1 (~70 %) than Tpm2.2 (~10 %) (Peng et al. 2013a) was observed while in this study swine skeletal muscles contained a similar amount of Tpm1.1 (~52 %); however, the expression level of Tpm2.2 (~44 %) was higher in skeletal muscle in comparison to that in cardiac tissue. In another study of Tpm isoforms in human heart, Tpm1.1 (~68 %) is the major isoform together with Tpm2.2 (~6 %) and Tpm1.2 (~2 %) as two minor isoforms (Peng et al. 2013b). In contrast, Tpm2.2 (~60 %) is the predominant isoform, while Tpm1.1 (~16 %) and Tpm3.12 (~24 %) are present in this study for human skeletal muscles. This result also agrees with Klitgaard et al.'s study using 2D gel electrophoresis, which showed human vastus lateralis contains higher amount of Tpm2.2 than Tpm1.1(Klitgaard et al. 1990). Moreover, our results show the Tpm2.2 is the major species in rat diaphragm and soleus, which agree with others previously reported (Carraro et al. 1981; Klitgaard et al. 1990). Given that the expression of different Tpm isoforms has been linked to altered contractility in muscle (Palmiter et al. 1996), differences in Tpm isoform composition between muscle types or across species may contribute to muscle type- or species-specific differences in contractile function.

Conclusions

Top-down MS was employed to comprehensively characterize Tpm isoforms in swine, rat, and human skeletal muscles with high reproducibility. The LC/MS+ strategy combining online LC/MS purification and offline top-down high-resolution MS is efficient in separating, detecting, and characterizing myofilament proteins without the use of specific antibodies or gel electrophoresis. In addition, top-down analysis directly detects intact proteins and, thus, provides a global view of all detectable protein isoforms and proteoforms in one spectrum without prior knowledge (Dhoot and Perry 1979). Sequence variants were assigned to the Tpm isoforms based on the high-resolution MS and MS/MS data. Compelling evidence shows the relative abundance of Tpm isoforms and their PTMs is muscle-type dependent among the species investigated (rat and human). Our results demonstrate that top-down LC/MS+ is a powerful tool for the comprehensive analysis of myofilament proteins in skeletal muscles and could potentially be further applied to study changes in Tpm protein isoforms in muscle-related diseases.

References

Arrell DK, Neverova I, Fraser H, Marban E, Van Eyk JE (2001) Proteomic analysis of pharmacologically preconditioned cardiomyocytes reveals novel phosphorylation of myosin light chain 1. Circ Res 89:480–487

Ayaz-Guner S, Zhang J, Li L, Walker JW, Ge Y (2009) In vivo phosphorylation site mapping in mouse cardiac troponin I by high resolution top-down electron capture dissociation mass spectrometry: Ser22/23 are the only sites basally phosphorylated. Biochemistry 48:8161–8170

Bailey K (1948) Tropomyosin: a new asymmetric protein component of the muscle fibril. Biochem J 43:271–279

Bottinelli R, Reggiani C (2000) Human skeletal muscle fibres: molecular and functional diversity. Prog Biophys Mol Bio 73:195–262

Brown JH, Kim KH, Jun G, Greenfield NJ, Dominguez R, Volkmann N, Hitchcock-DeGregori SE, Cohen C (2001) Deciphering the design of the tropomyosin molecule. Proc Natl Acad Sci USA 98:8496–8501

Canton M, Neverova I, Menabo R, Van Eyk J, Di Lisa F (2004) Evidence of myofibrillar protein oxidation induced by postischemic reperfusion in isolated rat hearts. Am J Physiol Heart Circ Physiol 286:H870–H877

Carraro U, Catani C, Libera LD, Vascon M, Zanella G (1981) Differential distribution of tropomyosin subunits in fast and slow rat muscles and its changes in long-term denervated hemidiaphragm. FEBS Lett 128:233–236

Chait BT (2006) Mass spectrometry: bottom-up or top-down? Science 314:65–66

Chen YC, Ayaz-Guner S, Peng Y, Lane NM, Locher MR, Kohmoto T, Larsson L, Moss RL, Ge Y (2015) Effective top-down LC/MS plus method for assessing actin isoforms as a potential cardiac disease marker. Anal Chem 87:8399–8406

Clarke NF, Domazetovska A, Waddell L, Kornberg A, McLean C, North KN (2009) Cap disease due to mutation of the beta-tropomyosin gene (TPM2). Neuromuscul Disord 19:348–351

Cummins P, Perry SV (1974) Chemical and immunochemical characteristics of tropomyosins from striated and smooth muscle. Biochem J 141:43–49

Denz CR, Narshi A, Zajdel RW, Dube DK (2004) Expression of a novel cardiac-specific tropomyosin isoform in humans. Biochem Bioph Res Co 320:1291–1297

Dhoot GK, Perry SV (1979) Distribution of polymorphic forms of troponin components and tropomyosin in skeletal-muscle. Nature 278:714–718

Dong XT, Sumandea CA, Chen YC, Garcia-Cazarin ML, Zhang J, Balke CW, Sumandea MP, Ge Y (2012) Augmented phosphorylation of cardiac troponin I in hypertensive heart failure. J Biol Chem 287:848–857

Driessen HPC, Dejong WW, Tesser GI, Bloemendal H (1985) The mechanism of N-terminal acetylation of proteins. Crit Rev Biochem Mol 18:281–325

Eliuk S, Makarov A (2015) Evolution of orbitrap mass spectrometry instrumentation. Annu Rev Anal Chem 8:61–80

El-Mezgueldi M, Asiri S, Albishri W, Nowak K (2014) Skeletal muscle myopathy mutations in tropomyosin gene TPM3 affect thin filament transitions between the inactive and active states. Biophys J 106:350a

Ge Y, Rybakova IN, Xu QG, Moss RL (2009) Top-down high-resolution mass spectrometry of cardiac myosin binding protein C revealed that truncation alters protein phosphorylation state. Proc Natl Acad Sci USA 106:12658–12663

Geeves MA, Hitchcock-DeGregori SE, Gunning PW (2015) A systematic nomenclature for mammalian tropomyosin isoforms. J Muscle Res Cell M 36:147–153

Greenfield NJ, Montelione GT, Farid RS, Hitchcock-DeGregori SE (1998) The structure of the N-terminus of striated muscle alpha-tropomyosin in a chimeric peptide: nuclear magnetic resonance structure and circular dichroism studies. Biochemistry 37:7834–7843

Guner H, Close PL, Cai WX, Zhang H, Peng Y, Gregorich ZR, Ge Y (2014) MASH suite: a user-friendly and versatile software interface for high-resolution mass spectrometry data interpretation and visualization. J Am Soc Mass Spectr 25:464–470

Gunning PW, Schevzov G, Kee AJ, Hardeman EC (2005) Tropomyosin isoforms: divining rods for actin cytoskeleton function. Trends Cell Biol 15:333–341

Gunning P, O'Neill G, Hardeman E (2008) Tropomyosin-based regulation of the actin cytoskeleton in time and space. Physiol Rev 88:1–35

Heeley DH, Dhoot GK, Frearson N, Perry SV, Vrbova G (1983) The effect of cross-innervation on the tropomyosin composition of rabbit skeletal muscle. FEBS Lett 152:282–286

Hendrickson CL, Quinn JP, Kaiser NK, Smith DF, Blakney GT, Chen T, Marshall AG, Weisbrod CR, Beu SC (2015) 21 tesla fourier transform ion cyclotron resonance mass spectrometer: a national resource for ultrahigh resolution mass analysis. J Am Soc Mass Spectr 26:1626–1632

Hitchcock-DeGregori SE, Heald RW (1987) Altered actin and troponin binding of amino-terminal variants of chicken striated-muscle alpha-tropomyosin expressed in *Escherichia coli*. J Biol Chem 262:9730–9735

Hitchcock-DeGregori SE, Huxley HE, Szent-Gyorgyi AG (1973) Calcium sensitive binding of troponin to actin-tropomyosin: a two-site model for troponin action. J Mol Biol 80:825–836

Holden DD, Mcgee WM, Brodbelt JS (2016) Integration of ultraviolet photodissociation with proton transfer reactions and ion parking for analysis of intact proteins. Anal Chem 88:1008–1016

Horn DM, Zubarev RA, McLafferty FW (2000) Automated reduction and interpretation of high resolution electrospray mass spectra of large molecules. J Am Soc Mass Spectr 11:320–332

Huang TY, McLuckey SA (2010) Top-down protein characterization facilitated by ion/ion reactions on a quadrupole/time of flight platform. Proteomics 10:3577–3588

Janco M, Suphamungmee W, Li XC, Lehman W, Lehrer SS, Geeves MA (2013) Polymorphism in tropomyosin structure and function. J Muscle Res Cell M 34:177–187

Jin JP, Lin JJC (1988) Rapid purification of mammalian cardiac troponin-T and its isoform switching in rat hearts during development. J Biol Chem 263:7309–7315

Johnson MA, Polgar J, Weightman D, Appleton D (1973) Data on the distribution of fibre types in thirty-six human muscles. An autopsy study. J Neurol Sci 18:111–129

Kee AJ, Hardeman EC (2008) Tropomyosins in skeletal muscle diseases. Adv Exp Med Biol 644:143–157

Klitgaard H, Mantoni M, Schiaffino S, Ausoni S, Gorza L, Laurentwinter C, Schnohr P, Saltin B (1990) Function, morphology and protein expression of aging skeletal-muscle: a cross-sectional study of elderly men with different training backgrounds. Acta Physiol Scand 140:41–54

Kostyukevich YI, Vladimirov GN, Nikolaev EN (2012) Dynamically harmonized FT-ICR cell with specially shaped electrodes for compensation of inhomogeneity of the magnetic field. Computer simulations of the electric field and ion motion dynamics. J Am Soc Mass Spectr 23:2198–2207

Lees-Miller JP, Helfman DM (1991) The molecular basis for tropomyosin isoform diversity. BioEssays 13:429–437

Marston SB, Redwood CS (2003) Modulation of thin filament activation by breakdown or isoform switching of thin filament proteins: physiological and pathological implications. Circ Res 93:1170–1178

Marston SB, Copeland O, Messer AE, MacNamara E, Nowak K, Zampronio CG, Ward DG (2013) Tropomyosin isoform expression and phosphorylation in the human heart in health and disease. J Muscle Res Cell M 34:189–197

Memo M, Marston S (2013) Skeletal muscle myopathy mutations at the actin tropomyosin interface that cause gain- or loss-of-function. J Muscle Res Cell M 34:165–169

Neverova I, Van Eyk JE (2002) Application of reversed phase high performance liquid chromatography for subproteomic analysis of cardiac muscle. Proteomics 2:22–31

Palmiter KA, Kitada Y, Muthuchamy M, Wieczorek DF, Solaro RJ (1996) Exchange of beta- for alpha-tropomyosin in hearts of transgenic mice induces changes in thin filament response to Ca^{2+} strong cross-bridge binding, and protein phosphorylation. J Biol Chem 271:11611–11614

Peng Y, Chen X, Sato T, Rankin SA, Tsuji RF, Ge Y (2012) Purification and high-resolution top-down mass spectrometric characterization of human salivary alpha-amylase. Anal Chem 84:3339–3346

Peng Y, Chen X, Zhang H, Xu QG, Hacker TA, Ge Y (2013a) Top-down targeted proteomics for deep sequencing of tropomyosin isoforms. J Proteome Res 12:187–198

Peng Y, Yu DY, Gregorich Z, Chen X, Beyer AM, Gutterman DD, Ge Y (2013b) In-depth proteomic analysis of human tropomyosin by top-down mass spectrometry. J Muscle Res Cell M 34:199–210

Peng Y, Gregorich ZR, Valeja SG, Zhang H, Cai WX, Chen YC, Guner H, Chen AJ, Schwahn DJ, Hacker TA, Liu XW, Ge Y (2014) Top-down proteomics reveals concerted Reductions in myofilament and Z-disc protein phosphorylation after acute myocardial infarction. Mol Cell Proteomics 13:2752–2764

Perry SV (2001) Vertebrate tropomyosin: distribution, properties and function. J Muscle Res Cell M 22:5–49

Pittenger MF, Kazzaz JA, Helfman DM (1994) Functional properties of non-muscle tropomyosin isoforms. Curr Opin Cell Biol 6:96–104

Rajan S, Jagatheesan G, Karam CN, Alves ML, Bodi I, Schwartz A, Bulcao CF, D'Souza KM, Akhter SA, Boivin GP, Dube DK, Petrashevskaya N, Herr AB, Hullin R, Liggett SB, Wolska BM, Solaro RJ, Wieczorek DF (2010) Molecular and functional characterization of a novel cardiac-specific human tropomyosin isoform. Circulation 121:410

Romeroherrera AE, Nasser S, Lieska NG (1982) Heterogeneity of adult human striated-muscle tropomyosin. Muscle Nerve 5:713–718

Scellini B, Piroddi N, Flint GV, Regnier M, Poggesi C, Tesi C (2015) Impact of tropomyosin isoform composition on fast skeletal muscle thin filament regulation and force development. J Muscle Res Cell M 36:11–23

Schevzov G, Vrhovski B, Bryce NS, Elmir S, Qiu MR, O'Neill GM, Yang N, Verrills NM, Kavallaris M, Gunning PW (2005) Tissue-specific tropomyosin isoform composition. J Histochem Cytochem 53:557–570

Schiaffino S, Reggiani C (2011) Fiber types in mammalian skeletal muscles. Physiol Rev 91:1447–1531

Scott W, Stevens J, Binder-Macleod SA (2001) Human skeletal muscle fiber type classifications. Phys Ther 81:1810–1816

Senko MW, Speir JP, Mclafferty FW (1994) Collisional activation of large multiply-charged ions using fourier-transform mass-spectrometry. Anal Chem 66:2801–2808

Smith LM, Kelleher NL, Proteomics CTD (2013) Proteoform: a single term describing protein complexity. Nat Methods 10:186–187

Tajsharghi H, Ohlsson M, Palm L, Oldfors A (2012) Myopathies associated with beta-tropomyosin mutations. Neuromuscul Disord 22:923–933

Thangaraj B, Ryan CM, Souda P, Krause K, Faull KF, Weber APM, Fromme P, Whitelegge JP (2010) Data-directed top-down fourier-transform mass spectrometry of a large integral membrane protein complex: photosystem II from *Galdieria sulphuraria*. Proteomics 10:3644–3656

Wang J, Thurston H, Essandoh E, Otoo M, Han MD, Rajan A, Dube S, Zajdel RW, Sanger JM, Linask KK, Dube DK, Sanger JW (2008) Tropomyosin expression and dynamics in developing avian embryonic muscles. Cell Motil Cytoskel 65:379–392

Whitelegge JP, Zhang HM, Aguilera R, Taylor RM, Cramer WA (2002) Full subunit coverage liquid chromatography electrospray ionization mass spectrometry (LCMS+) of an oligomeric membrane protein: cytochrome b6f complex from spinach and the cyanobacterium *Mastigocladus laminosus*. Mol Cell Proteomics 1:816–827

Wieczorek DF, Smith CW, Nadal-Ginard B (1988) The rat alpha-tropomyosin gene generates a minimum of six different mRNAs

coding for striated, smooth, and nonmuscle isoforms by alternative splicing. Mol Cell Biol 8:679–694

Xian F, Hendrickson CL, Marshall AG (2012) High resolution mass spectrometry. Anal Chem 84:708–719

Zabrouskov V, Ge Y, Schwartz J, Walker JW (2008) Unraveling molecular complexity of phosphorylated human cardiac troponin I by top down electron capture dissociation/electron transfer dissociation mass spectrometry. Mol Cell Proteomics 7:1838–1849

Zubarev RA, Horn DM, Fridriksson EK, Kelleher NL, Kruger NA, Lewis MA, Carpenter BK, McLafferty FW (2000) Electron capture dissociation for structural characterization of multiply charged protein cations. Anal Chem 72:563–573